Supplementary Materials

A mono-oxo-bridged binuclear iron(III) complex with a Fe-O-Fe angle of 180.0° and its catalytic activity for hydrogen evolution

Xia-Xing Sun, Juan Du, Jie-Jie Tan and Shu-Zhong Zhan*

College of Chemistry and Chemical Engineering, South China University of Technology, Guangzhou 510640, China

Table of Contents

9	**Fig. S8.** Cyclic voltammograms of 0.516 mM [(H_2O)(bpc)Fe-O-Fe(bpc)(H_2O)], or $FeCl_3$ in 0.10 M of [*n*-Bu_4N]ClO_4 CH_3CN solution at a glassy carbon electrode and a scan rate of 100 mV/s, $Ag/AgNO_3$ reference electrode, Fc internal standard (*).
10	**Fig. S9.** Scan rate dependence of precatalytic waves for a 5.16 mM solution of [(H_2O)(bpc)Fe-O-Fe(bpc)(H_2O)] (0.10 M [*n*-Bu_4N]ClO_4), at scan rates from 50 to 300 mV/s.
11	**Fig. S10.** Cyclic voltammograms of [(H_2O)(bpc)Fe-O-Fe(bpc)(H_2O)] (1.2 mM) with varying scan rate in 0.10 M of [n-Bu_4N]ClO_4 DMF solution at a glassy carbon electrode and $Ag/AgNO_3$ reference electrode, Fc internal standard (*).
12	**Fig. S11.** Cyclic voltammograms of [(H_2O)(bpc)Fe-O-Fe(bpc)(H_2O)] (1.2 mM) with 0.67 mM acetic acid at varying scan rate in 0.10 M of [n-Bu_4N]ClO_4 DMF solution at a glassy carbon electrode and $Ag/AgNO_3$ reference electrode, Fc internal standard (*).
13	**Fig. S12.** Cyclic voltammograms of [(H_2O)(bpc)Fe-O-Fe(bpc)(H_2O)] (1.2 mM) with 1.0 mM acetic acid at varying scan rate in 0.10 M of [n-Bu_4N]ClO_4 DMF solution at a glassy carbon electrode and $Ag/AgNO_3$ reference electrode, Fc internal standard (*).
14	**Fig. S13.** Cyclic voltammograms of [(H_2O)(bpc)Fe-O-Fe(bpc)(H_2O)] (1.2 mM) with 1.33 mM acetic acid at varying scan rate in 0.10 M of [n-Bu_4N]ClO_4 DMF solution at a glassy carbon electrode and $Ag/AgNO_3$ reference electrode, Fc internal standard (*).
15	**Fig. S14.** Cyclic voltammograms of *[(H_2O)(bpc)Fe-O-Fe(bpc)(H_2O)]* (1.2 mM) with 1.67 mM acetic acid at varying scan rate in 0.10 M of [*n*-Bu_4N]ClO_4 DMF solution at a glassy carbon electrode and $Ag/AgNO_3$ reference electrode, Fc internal standard (*).

16	**Fig. S15.** Cyclic voltammograms of [(H_2O)(bpc)Fe-O-Fe(bpc)(H_2O)] (1.2 mM) with 2.50 mM acetic acid at varying scan rate in 0.10 M of [n-Bu_4N]ClO_4 DMF solution at a glassy carbon electrode and Ag/$AgNO_3$ reference electrode, Fc internal standard (*).
17	**Fig. S16.** Cyclic voltammograms of [(H_2O)(bpc)Fe-O-Fe(bpc)(H_2O)] (1.2 mM) with 3.30 mM acetic acid at varying scan rate in 0.10 M of [n-Bu_4N]ClO_4 DMF solution at a glassy carbon electrode and Ag/$AgNO_3$ reference electrode, Fc internal standard (*).
18	**Fig. S17.** ^{1}H NMR spectra of a DMSO solution of (a) 0.598 mM [(H_2O)(bpc)Fe-O-Fe(bpc)(H_2O)]; (b) 0.598 mM [(H_2O)(bpc)Fe-O-Fe(bpc)(H_2O)] with 0.025 M acetic acid; (c) 0.025 M acetic acid.
19	**Fig. S18.** UV-Vis spectra of a DMF solution of 0.598 mM [(H_2O)(bpc)Fe-O-Fe(bpc)(H_2O)] with or without acetic acid (14.1 mM).

Physical measurements

IR spectra were obtained as KBr pellets on a Bruker 1600 FT-IR spectrometer from 4000 to 400 cm^{-1}. NMR analyses were carried out by using a Bruker AV-500 instrument. UV-vis spectra were measured on a Hitachi U-3010. Measurements and analyses for the chemical compositions and valence states of the photocatalysts were carried out by ESCALAB 250 Xi X-photoelectron spectroscopy (XPS) with monochromatic Al Kα (1486.6 eV) X-ray sources. A Quantum Design SQUID Magnetometer MPMS XL-7 was used to investigate magnetic behavior of the iron complex. ESR spectra of the iron complex were taken on a Bruker Elexsys II E500 ESR spectrometer. Mössbauer spectrum of [(H_2O)(bpc)Fe-O-Fe(bpc)(H_2O)] was measured on a Wss-10 Mössbauer spectrometer. Electrochemical measurements and

analysis were conducted by using a CHI-660E electrochemical analyzer using a three-electrode cell in which a glassy carbon electrode (1 mm in diameter) is the working electrode, a saturated $Ag/AgNO_3$ electrode is the reference electrode, and a platinum wire is the auxiliary electrode. For organic media, 0.10 M $[(n\text{-}Bu)_4N]ClO_4$ was selected as a supporting electrolyte.

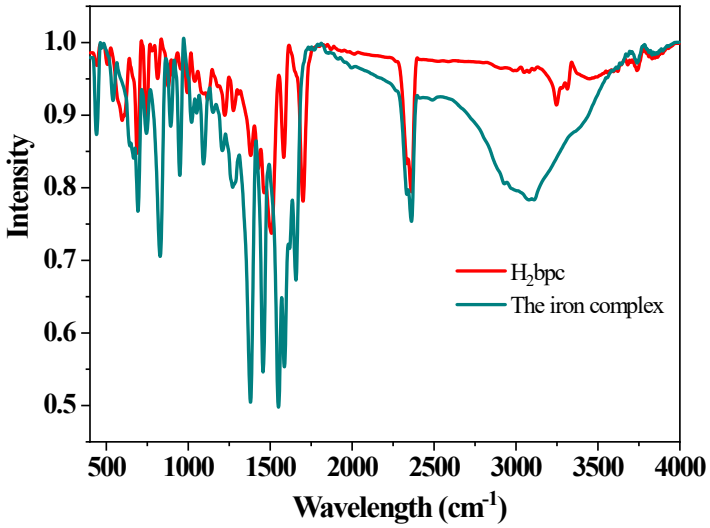

Fig. S1. IR spectra of the ligand, H_2bpc, and the iron complex, $[(H_2O)(bpc)Fe\text{-}O\text{-}Fe(bpc)(H_2O)]$.

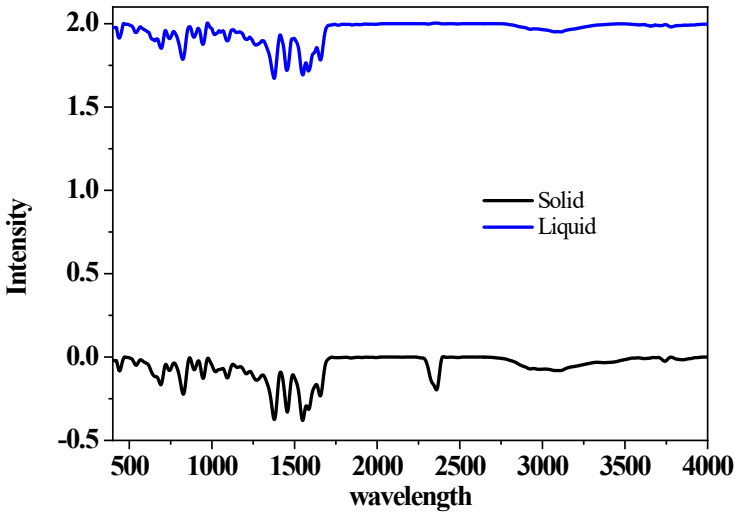

Fig. S2. IR spectra of the iron complex in solid and in DMF (0.05 M).

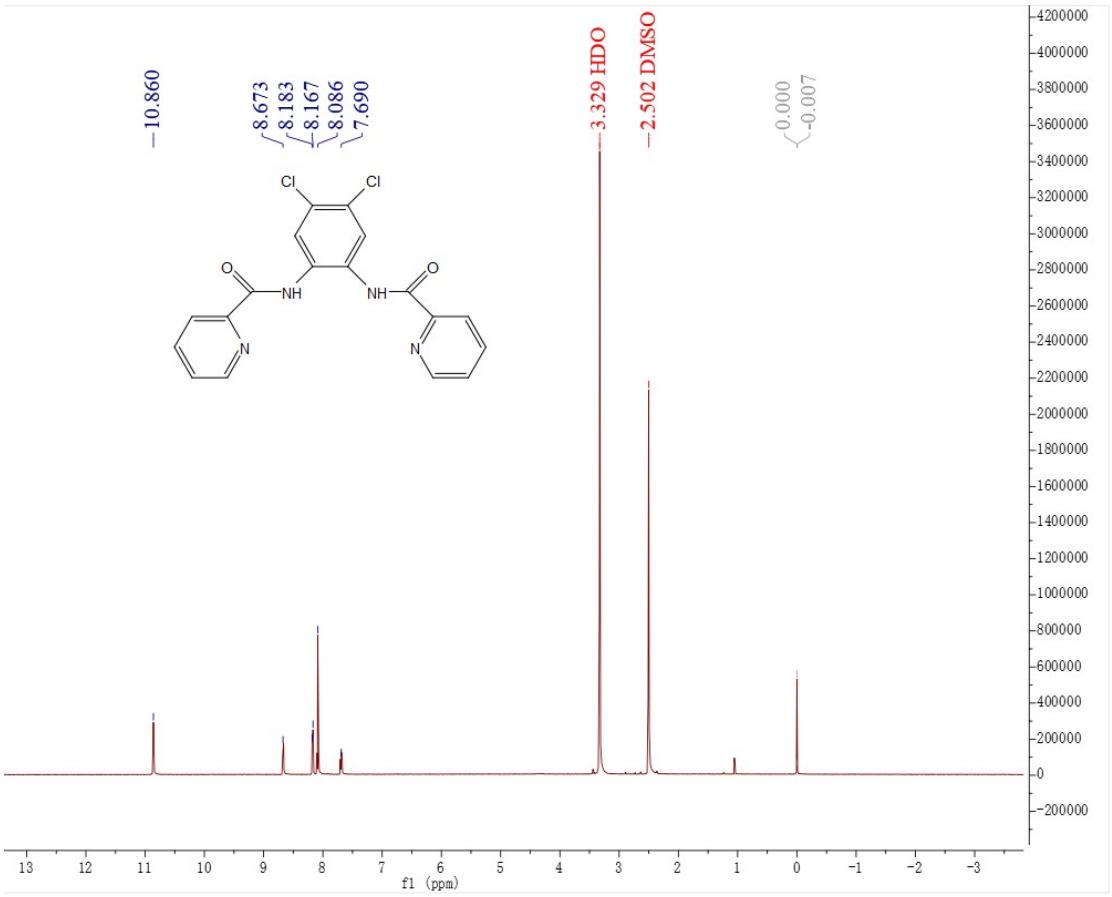

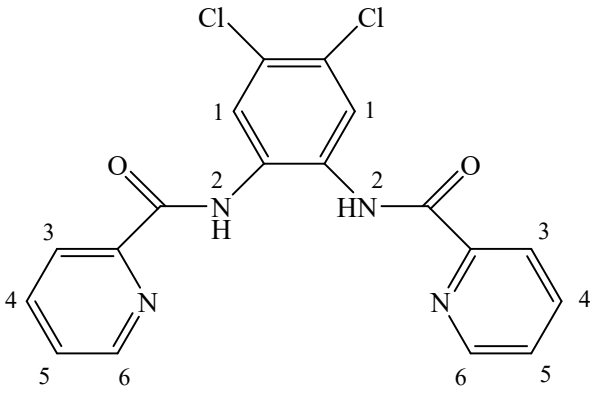

Fig. S3. ^{1}H NMR spectrum of the ligand, H_2bpc in DMSO. 1) 7.690 ppm; 2) 10.860 ppm; 3) 8.813 ppm; 4) 8.167 ppm; 5) 8.086 ppm; 6) 8.673 ppm.

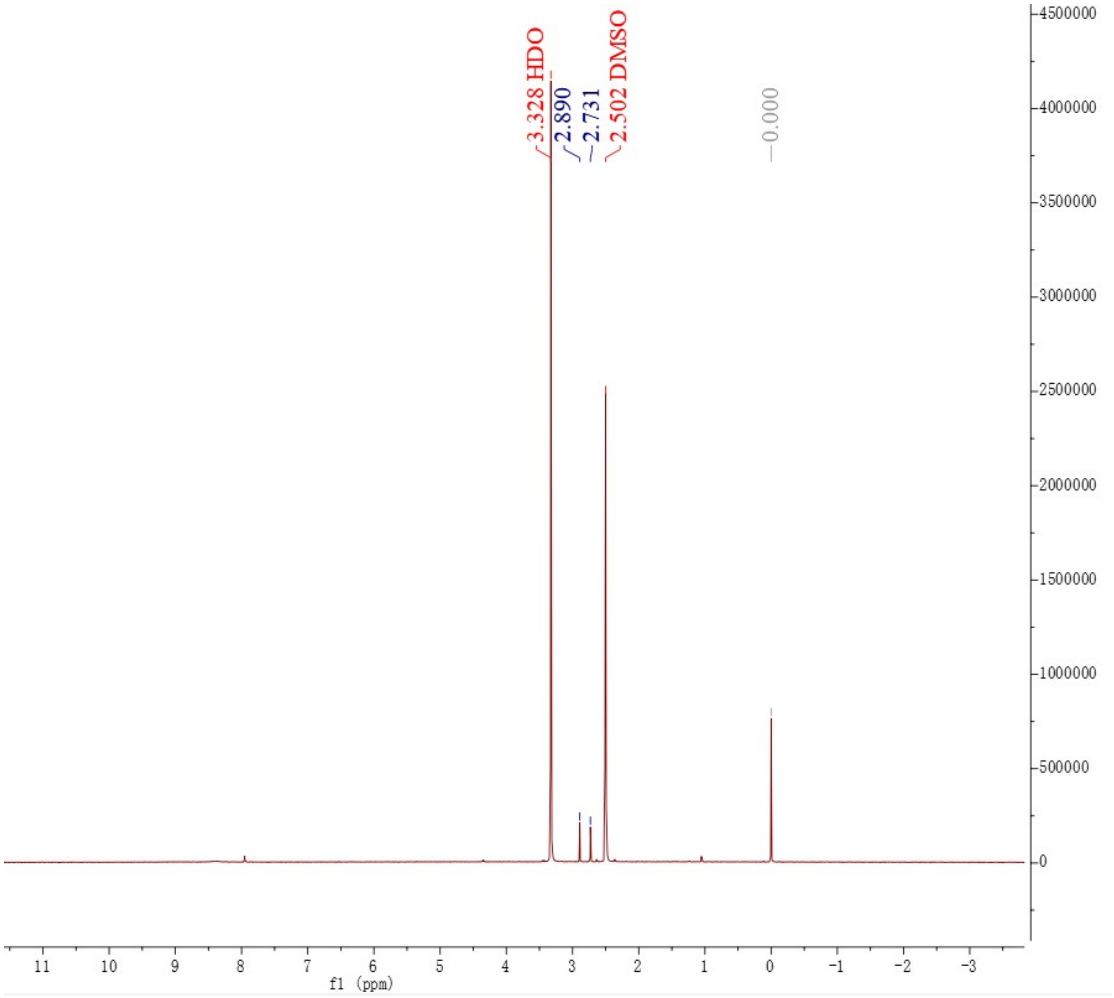

Fig. S4. ^{1}H NMR spectrum of the iron complex in DMSO.

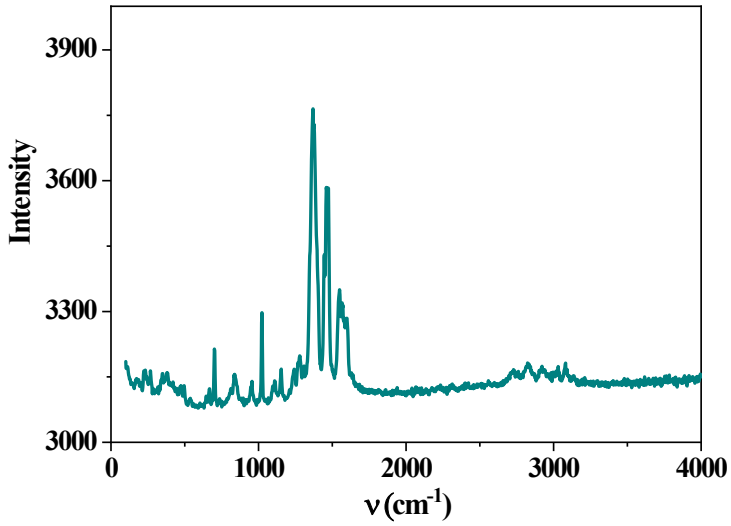

Fig. S5. Raman spectra of the iron complex.

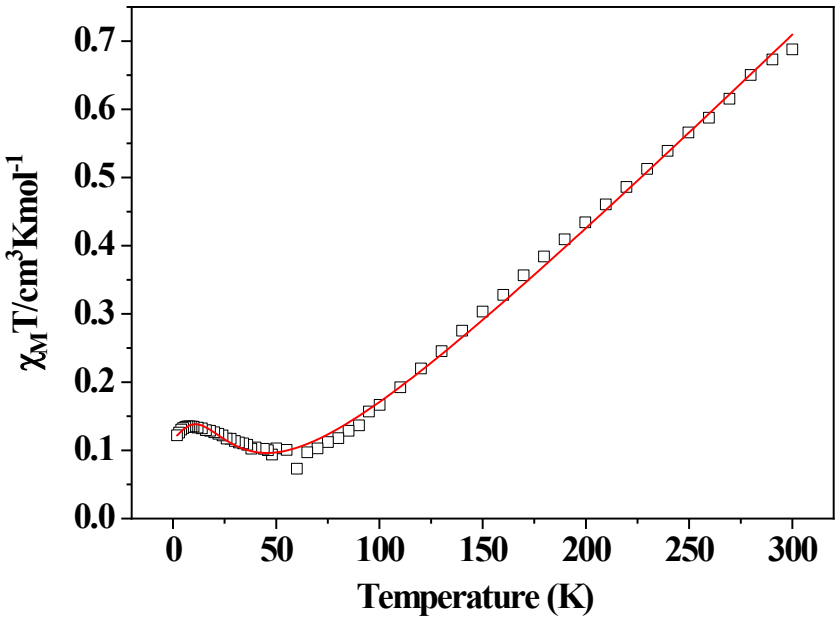

Fig. S6. Magnetic behavior of [(H_2O)(bpc)Fe-O-Fe(bpc)(H_2O)] under varying temperature. The solid line represents the result of the fitting of the parameters of Eq. (1) with the data.

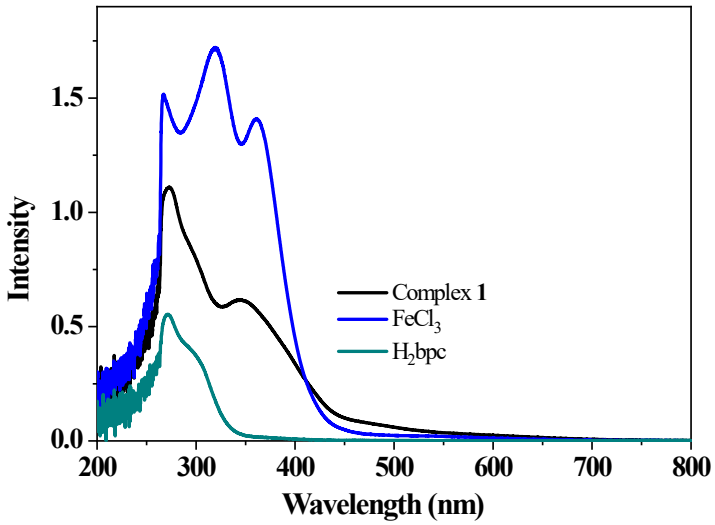

Fig. S7. UV-Vis spectra of the iron complex (0.235 mM), H_2bpc (0.235 mM) and $FeCl_3$ (0.235 mM) in DMF.

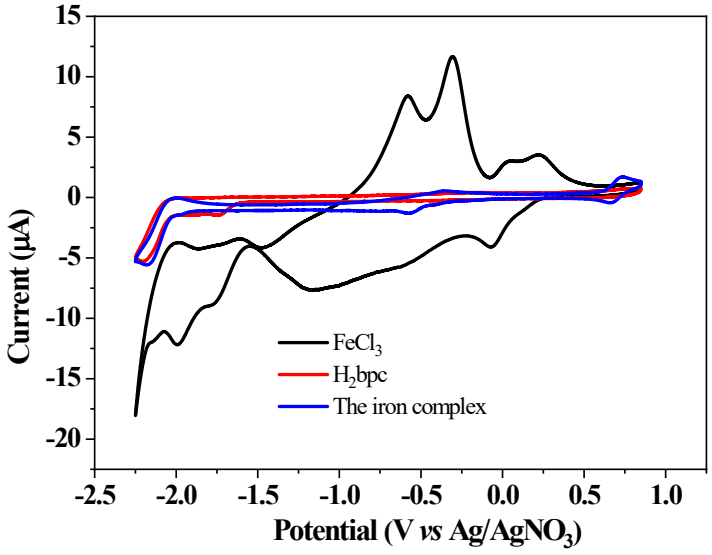

Fig. S8. Cyclic voltammograms of 0.516 mM $[(H_2O)(bpc)Fe\text{-}O\text{-}Fe(bpc)(H_2O)]$, or $FeCl_3$ in 0.10 M of $[n\text{-}Bu_4N]ClO_4$ CH_3CN solution at a glassy carbon electrode and a scan rate of 100 mV/s, $Ag/AgNO_3$ reference electrode, Fc internal standard (*).

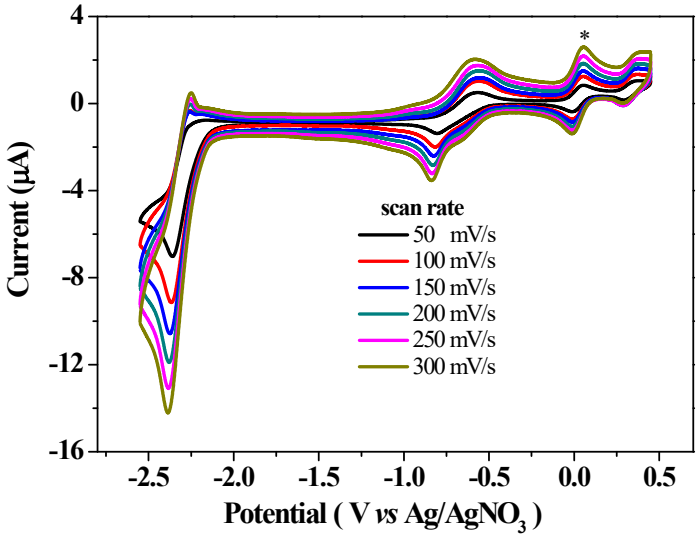

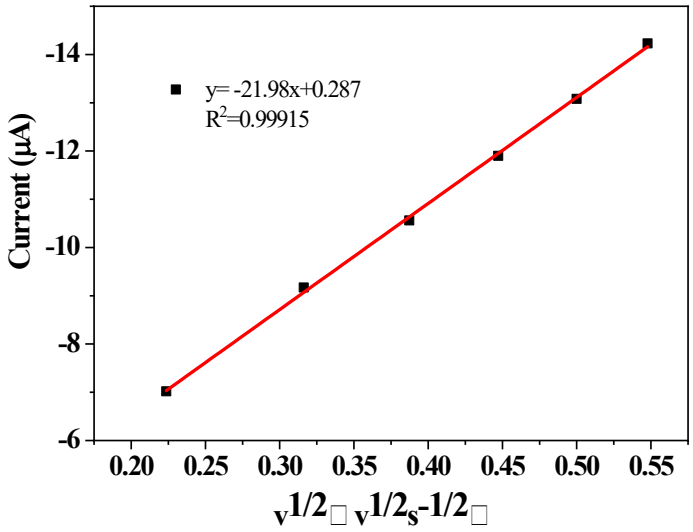

Fig. S9. Scan rate dependence of precatalytic waves for a 5.16 mM solution of [(H_2O)(bpc)Fe-O-Fe(bpc)(H_2O)] (0.10 M [*n*-Bu_4N]ClO_4), at scan rates from 50 to 300 mV/s.

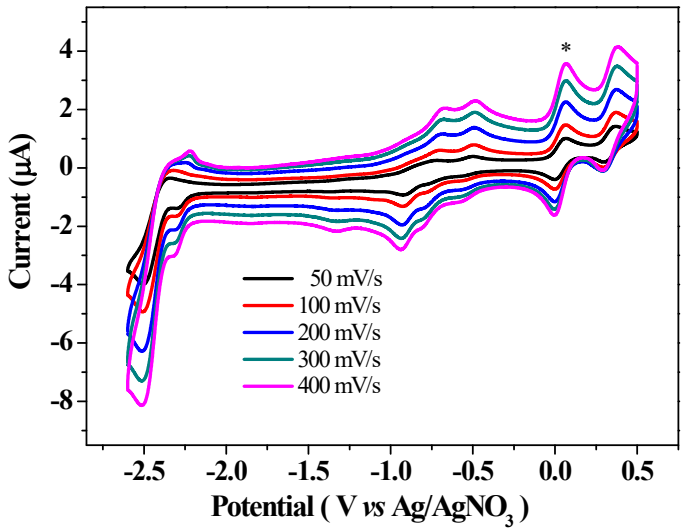

Fig. S10. Cyclic voltammograms of [(H_2O)(bpc)Fe-O-Fe(bpc)(H_2O)] (1.2 mM) with varying scan rate in 0.10 M of [n-Bu_4N]ClO_4 DMF solution at a glassy carbon electrode and $Ag/AgNO_3$ reference electrode, Fc internal standard (*).

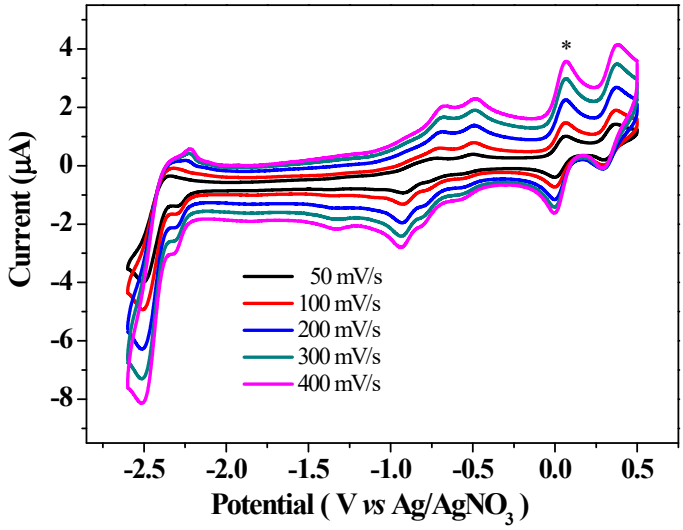

Fig. S11. Cyclic voltammograms of $[(H_2O)(bpc)Fe\text{-}O\text{-}Fe(bpc)(H_2O)]$ (1.2 mM) with 0.67 mM acetic acid at varying scan rate in 0.10 M of $[n\text{-}Bu_4N]ClO_4$ DMF solution at a glassy carbon electrode and $Ag/AgNO_3$ reference electrode, Fc internal standard (*).

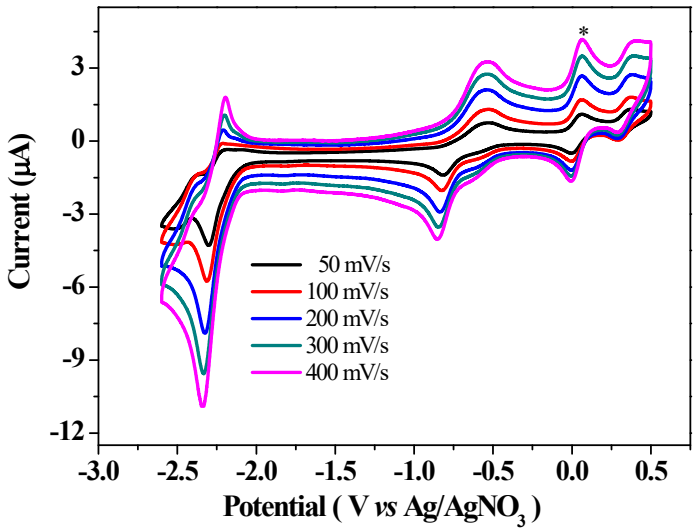

Fig. S12. Cyclic voltammograms of $[(H_2O)(bpc)Fe\text{-}O\text{-}Fe(bpc)(H_2O)]$ (1.2 mM) with 1.0 mM acetic acid at varying scan rate in 0.10 M of $[n\text{-}Bu_4N]ClO_4$ DMF solution at a glassy carbon electrode and $Ag/AgNO_3$ reference electrode, Fc internal standard (*).

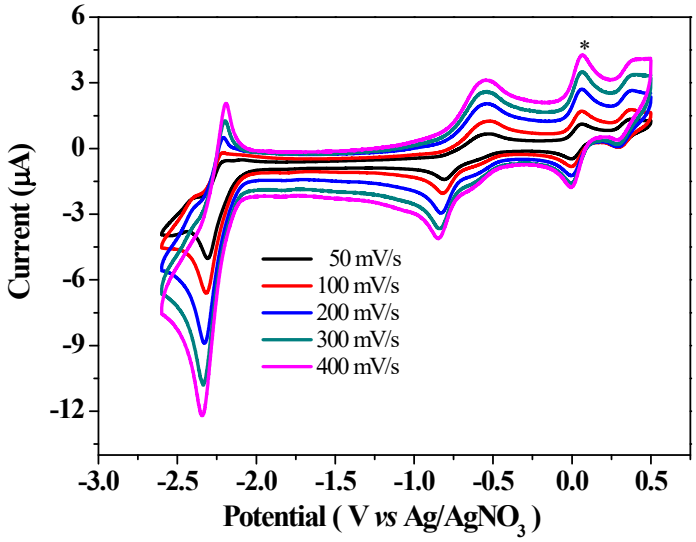

Fig. S13. Cyclic voltammograms of $[(H_2O)(bpc)Fe\text{-}O\text{-}Fe(bpc)(H_2O)]$ (1.2 mM) with 1.33 mM acetic acid at varying scan rate in 0.10 M of $[n\text{-}Bu_4N]ClO_4$ DMF solution at a glassy carbon electrode and $Ag/AgNO_3$ reference electrode, Fc internal standard (*).

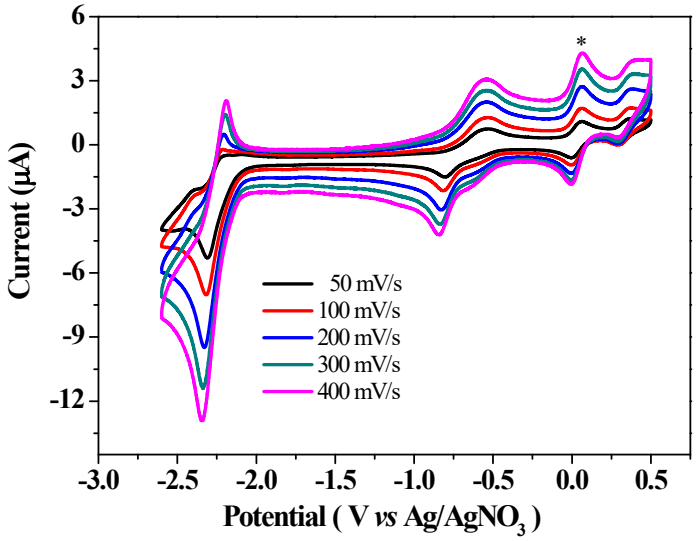

Fig. S14. Cyclic voltammograms of *$[(H_2O)(bpc)Fe\text{-}O\text{-}Fe(bpc)(H_2O)]$* (1.2 mM) with 1.67 mM acetic acid at varying scan rate in 0.10 M of $[n\text{-}Bu_4N]ClO_4$ DMF solution at a glassy carbon electrode and $Ag/AgNO_3$ reference electrode, Fc internal standard (*).

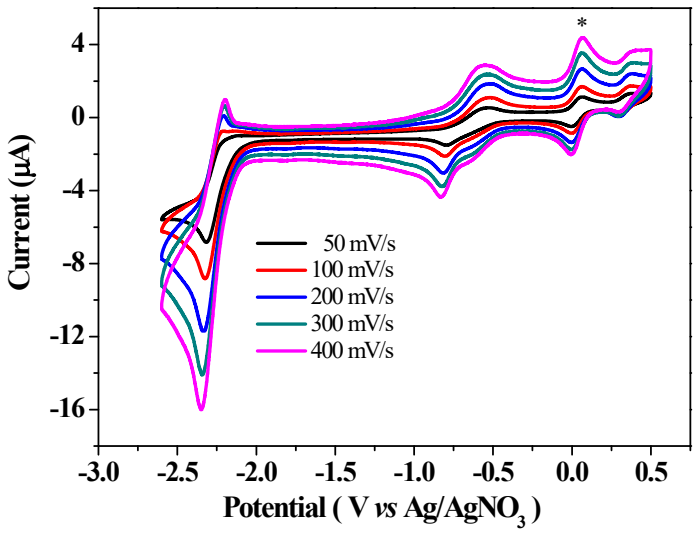

Fig. S15. Cyclic voltammograms of [(H_2O)(bpc)Fe-O-Fe(bpc)(H_2O)] (1.2 mM) with 2.50 mM acetic acid at varying scan rate in 0.10 M of [n-Bu_4N]ClO_4 DMF solution at a glassy carbon electrode and $Ag/AgNO_3$ reference electrode, Fc internal standard (*).

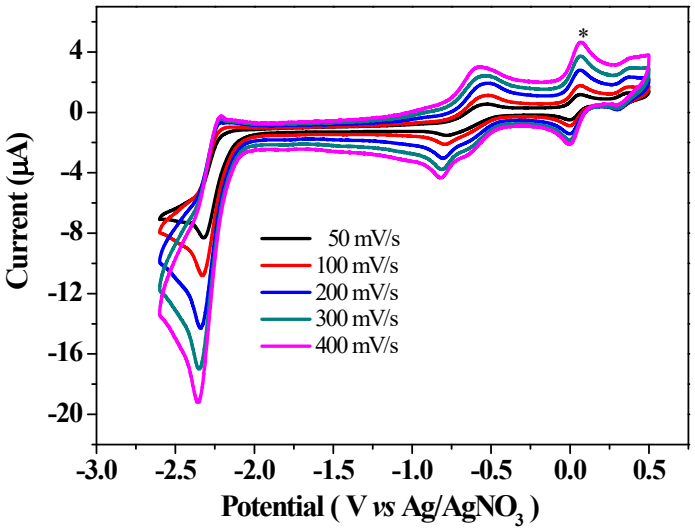

Fig. S16. Cyclic voltammograms of [(H_2O)(bpc)Fe-O-Fe(bpc)(H_2O)] (1.2 mM) with 3.30 mM acetic acid at varying scan rate in 0.10 M of [n-Bu_4N]ClO_4 DMF solution at a glassy carbon electrode and $Ag/AgNO_3$ reference electrode, Fc internal standard (*).

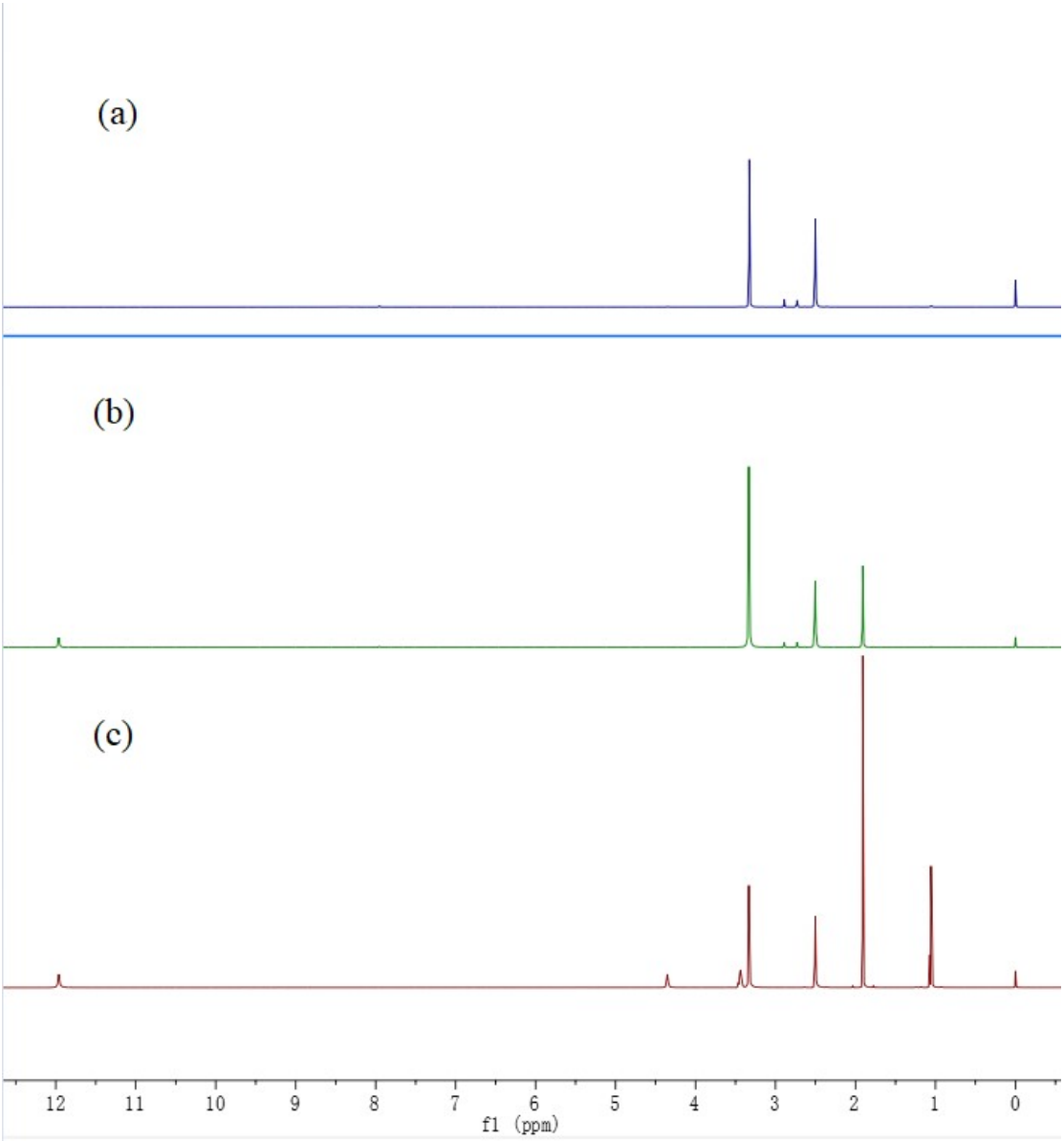

Fig. S17. ^{1}H NMR spectra of a DMSO solution of (a) 0.598 mM [(H_2O)(bpc)Fe-O-Fe(bpc)(H_2O)]; (b) 0.598 mM [(H_2O)(bpc)Fe-O-Fe(bpc)(H_2O)] with 0.025 M acetic acid; (c) 0.025 M acetic acid.

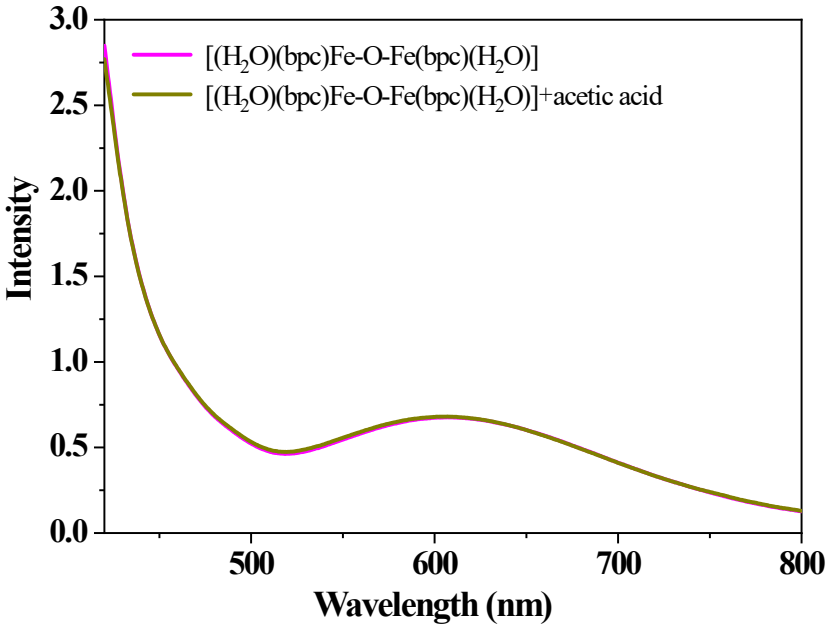

Fig. S18. UV-Vis spectra of a DMF solution of 0.598 mM [(H_2O)(bpc)Fe-O-Fe(bpc)(H_2O)] with or without acetic acid (14.1 mM).